Geomorphology 190 (2013) 27–39

Contents lists available at SciVerse ScienceDirect

Geomorphology

journal homepage: www.elsevier.com/locate/geomorph

Genesis of an esker-like ridge over the southern Fraser Plateau, British Columbia: Implications for paleo-ice sheet reconstruction based on geomorphic inversion

Andrew J. Perkins *, Tracy A. Brennand, Matthew J. Burke [1]

Department of Geography, Simon Fraser University, 8888 University Drive, Burnaby, BC, Canada V5A 1S6

ARTICLE INFO

Article history:
Received 30 April 2012
Received in revised form 6 February 2013
Accepted 11 February 2013
Available online 19 February 2013

Keywords:
Esker
Geomorphic inversion
Cordilleran Ice Sheet
Ground penetrating radar
Electrical resistivity tomography

ABSTRACT

Robust interpretations of meltwater systems operating during ice sheet decay are integral to reconstructing deglacial patterns and style. Yet over reliance on meltwater landform morphology with limited attention to morpho-sedimentary relationships, and basin-scale geomorphic and stratigraphic context can lead to unreliable geomorphic inversion-based paleo-ice sheet reconstructions. This problem is illustrated by the evolution of Young Lake esker-like ridge (YLER) formed in the Young Lake basin (YLB) on BC's southern Fraser Plateau during decay of the last Cordilleran Ice Sheet (CIS). We integrate data from digital elevation models, aerial photographs, sedimentary outcrops, water wells and shallow geophysics (ground-penetrating radar, electrical resistivity tomography). Previous interpretations of YLER as both an esker and an ice-contact, poorly-sorted, stratified deposit emplaced by westerly flowing meltwater, imply an eastward retreating ice margin. Geophysical data from a flat-topped component of YLER reveal slipface and planar-bedded sand and gravel overlying lacustrine sediments, characteristic of a Hjulstrom delta. Eastward-dipping foresets in a Gilbert delta exist at the eastern terminus. Contextually our observations suggest, despite esker-like morphology, YLER was not deposited within a subglacial ice tunnel. Instead, it formed through deposition of subaerial outwash between and/or on dead ice in front of a regionally backwasting ice margin. The complex deglacial evolution of YLB, including a drainage reversal and formation of two glacial lakes, supports northwestward backwasting of the CIS and dead ice within YLB. We conclude that accurate geomorphic inversion of meltwater landforms for deglacial paleo-ice sheet reconstruction requires knowledge of landform-scale morpho-sedimentary relationships and basin-scale geomorphic and stratigraphic context.

© 2013 Elsevier B.V. All rights reserved.

1. Introduction

Paleo-ice sheet reconstructions from geomorphic inversion (the use of the palimpsest glacial landforms such as till lineations, eskers, and meltwater channels to establish time-slice reconstructions of ice sheet properties and patterns) typically make assumptions about glacial landform genesis (e.g., Kleman and Borgstrom, 1996; Greenwood and Clark, 2009; Kleman et al., 2010). Accurate reconstructions of ice sheet growth and decay at the regional to local scale, therefore, rely heavily on the correct identification of landforms and their associated paleoglacial implications. Eskers form synchronously or time-transgressively in subglacial or englacial ice tunnels, or in supraglacial or ice-marginal ice-walled channels (Price, 1966; Banerjee and McDonald, 1975; Shreve, 1985; Hebrand and Åmark, 1989). Although these different formative environments reflect different deglacial styles and patterns (Shilts et al., 1987; Warren and Ashley, 1994; Brennand, 2000), subclassification of eskers along these lines (e.g., Warren and Ashley, 1994) has been rarely attempted. Rather, glacial geomorphic inversions aimed at deglacial paleo-ice sheet reconstruction have typically mapped esker ridges and assumed that all eskers formed time-transgressively near the ice margin during ice sheet decay despite some sedimentologically- and geophysically-based studies to the contrary (e.g., Brennand, 1994; Burke et al., 2012). It is our assertion that the accuracy of paleo-ice sheet reconstructions is often compromised when such reconstructions are derived from geomorphic inversions that rely solely on rudimentary landform identification, and assume landform genesis with little corroborating evidence.

The deglacial record of the last Cordilleran Ice Sheet (CIS) is replete with meltwater landforms (Tipper, 1971a,b,c; Kleman et al., 2010) and sediments (Ryder et al., 1991; Clague, 2000). However, their classification and interpretation is typically too general to allow accurate reconstruction of the pattern and style of paleo-ice sheet decay. This is, in part, because many landforms are heavily forested or relatively inaccessible by road, and consequently there is scant knowledge of their composition and morpho-sedimentary architecture. In addition, basin-scale geomorphic and stratigraphic records of deglacial events contained in basins set within the plateau surface have rarely been exploited (e.g., Plouffe et al., 2011). Here we

* Corresponding author. Tel.: +1 778 782 6812; fax: +1 778 782 5841.
E-mail addresses: ajp7@sfu.ca (A.J. Perkins), tabrenna@sfu.ca (T.A. Brennand), mjburke@liverpool.ac.uk (M.J. Burke).
[1] Present address: School of Environmental Sciences, Roxby Building, University of Liverpool, Liverpool, L69 7ZT, UK.

0169-555X/$ – see front matter © 2013 Elsevier B.V. All rights reserved.
http://dx.doi.org/10.1016/j.geomorph.2013.02.005

explore the morphology, composition and sedimentary architecture of one meltwater landform, an esker-like ridge within Young Lake basin, BC (Fig. 1B), placing it within the context of regional stratigraphy and basin evolution. We demonstrate that the integration of landform- and basin-scale data from digital elevation models (DEMs), aerial photographs, sedimentary outcrops, water wells and shallow geophysics (ground-penetrating radar, GPR; electrical resistivity tomography, ERT) allow more confident interpretations of landform genesis and thence deglacial style and pattern. We argue that such data integration should be integral to geomorphic inversion aimed at accurate paleo-ice sheet reconstructions, at least based on our present understanding of the general relationships between esker morpho-sedimentary character and formative process (and hence paleoglaciological implications).

1.1. Study area and previous work

Young Lake basin is located at the northeastern end of the Bonaparte valley on the southern Fraser Plateau of BC's south-central interior (Holland, 1976; Fig. 1A and B). The basin incorporates the Young Lake esker-like ridge (YLER), modern Young Lake, the upper Bonaparte and Rayfield Rivers as well as the unnamed creek draining north from Deadman valley and is contiguous with the lower Bonaparte River to the SW (Fig. 1A). The southern Fraser Plateau surface ranges from 1200 to 1800 m asl and is bordered on the west by the Coast Mountains and on the east by the Shuswap Highlands and Columbia Ranges. The relatively flat surface of the Fraser Plateau is a reflection of its underlying geology: successive basalt flows, dating to the late Eocene to Miocene (Bevier, 1983; Andrews and Russell, 2008). The plateau surface is generally mantled by a thin unit of till that is streamlined in places (Fig. 1B, streamline orientations roughly align NW–SE; Tipper, 1971a, b,c; Plouffe et al., 2011). Where basalt bedrock protrudes through the thin till cover, it displays one to two striae sets (Fig. 1A). Striae sets, streamlined bedforms, and till geochemistry have been used to reconstruct the evolution of ice flow direction for the last CIS (Plouffe et al., 2011). Initial ice advance onto the Fraser Plateau was from accumulation centers in the east (Tipper, 1971a,b). As westward-flowing ice accumulated on the plateau, it encountered eastward-flowing ice from the Coast Mountains, somewhere in the vicinity of the Fraser River valley (Heginbottom, 1972). This convergence resulted in ice flow diversion to the north and south (Tipper, 1971a,b). Late stage ice flow in the vicinity of YLER was to the SE (Plouffe et al., 2011; Fig. 1A).

Decay of the southern interior sector of the last CIS is thought to have occurred through a complex process dominated by downwasting, accompanied by limited backwasting of the ice margin from south to north (Tipper, 1971a; Fulton, 1991). On the Fraser Plateau the deglacial landform record includes meltwater channels, eskers, outwash sediments, hummocky deposits, minor moraine ridges, and glaciolacustrine sediments, including deltas and lake-bottom sediments (Tipper, 1971c; Bednarski, 2009; Huscroft, 2009; Plouffe, 2009). Ice-marginal positions are poorly known (indeed a clear pattern of deglacial retreat has been confounded by the lack of large recessional end moraines, Fulton, 1991; Plouffe et al., 2011) yet may be defined by meltwater landforms through geomorphic inversion, if the landforms are accurately classified. A genetic classification of eskers in the region is presently lacking, in part because poor access, forest cover and shallow sediment exposures (typically <1 m high) has limited the development of form-process models.

1.1.1. Young Lake esker-like ridge (YLER)

The YLER was initially classified as an esker or esker complex by Tipper (1971c) with formative paleoflow direction from east to west. Owen (1997) suggests that positive identification of a true esker be left to situations where geomorphology, sedimentology, and regional setting are all well understood. Perhaps with this in mind, and because few sedimentary exposures exist to confirm its sedimentary architecture, Plouffe (2009) conservatively interpreted the landform as an ice-contact, poorly-sorted, stratified deposit. Based on regional meltwater interpretations and the broad surface slope of glaciofluvial sediments within the Young Lake basin, paleoflow was inferred from east to west.

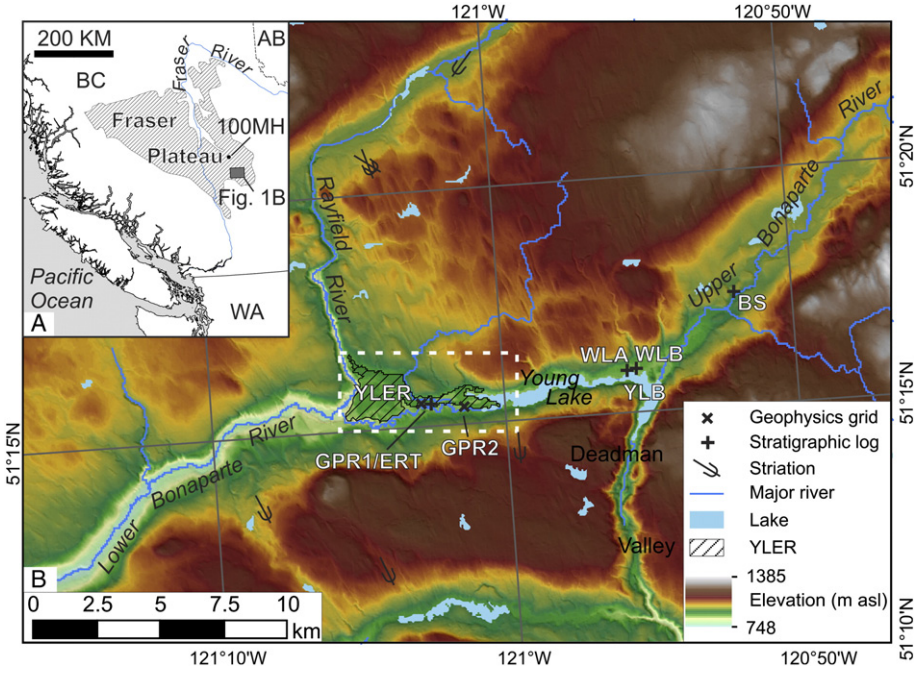

Fig. 1. (A) Location of the study area (Fig. 1B) on the Fraser Plateau (hash-marked polygon), and south of 100 Mile House (100MH). (B) Shaded DEM of Young Lake basin and surrounding plateau area (Geobase®). Young Lake basin is centered over modern Young Lake, incorporates Deadman Valley, upper Bonaparte River, Rayfield River, Young Lake esker-like ridge (YLER), and is contiguous with the lower Bonaparte River. The locations of ground-penetrating radar grid 1 (GPR1) and 2 (GPR2), the electrical resistivity tomography (ERT) line, well logs A (WLA) and B (WLB), and the Bonaparte section (BS) in Young Lake basin are shown. White dashed box indicates extent of Fig. 2B. Striae data are from Bednarski (2009) and Plouffe (2009).

2. Methods

The evolution of Young Lake basin and the genesis of the YLER were investigated by combining detailed geomorphic mapping and shallow geophysics on local ridge segments within the context of regional stratigraphy. Stereographic aerial photographs (1:40,000), regional digital elevation models (DEMs) (25-m resampled horizontal resolution, 10-m vertical resolution, Geobase®), and local DEMs generated from real-time kinematic (RTK) differential global positioning system (dGPS) measurements (Leica System 500, decimeter accuracy) were used for geomorphic mapping. An average systematic elevation offset of 13 m between elevation data collected directly from dGPS measurements and Geobase® DEM elevations in the field area resulted in the adjustment of all measurements in this study to local dGPS elevations. The landform elements of the YLER are characterized based on their surface morphology and relative relief. Geomorphic interpretations are supplemented by field observation of available sedimentary exposures and surface materials.

Shallow geophysical techniques were employed to delineate the sedimentary architecture and composition of the YLER. Two pseudo three-dimensional (3D) grids of 100 MHz GPR data (totaling ~2.3 km in linear distance) were collected. Grid 1 was collected on a relatively undisturbed, flat-topped segment of the YLER (Fig. 1B), whereas grid 2 was collected in a gravel pit (Fig. 1B) where 3–4 m of surface material had been excavated (except for the very edges of the pit). Data collection occurred with the antennas co-polarized, perpendicular broadside to the survey lines using a Sensors and Software Inc. pulseEKKO Pro system. During common offset (CO) surveys, antennas were kept at a constant separation of 1 m and data were collected in step mode (0.25 m). Two common mid-point (CMP) surveys provide an estimated average subsurface velocity of 0.107 ± 0.004 m/ns, which was used for data processing and to convert two-way travel time (TWTT) into depth. Processing of GPR data was completed in REFLEXW v5.6 and included time zero correction, low pass and bandpass filtering, migration, background removal, the application of a gain function, and topographic correction. Offsets in GPR reflections are interpreted as faults associated with removal (melting) of ice support (cf. Fiore et al., 2002). However, the full extent of faults (relative to landform thickness) may not be imaged owing to variations in fault orientation (relative to GPR survey direction) and GPR resolution. Elevation data for topographic correction was collected with an RTK dGPS. Data were collected in grids allowing for confident interpretation of bounding surfaces that could be traced throughout the grid; however, only those GPR lines sufficient to illustrate representative architectural forms are presented in this paper.

Two-dimensional (2D) ERT data were collected in a west–east orientation along the landform at GPR grid 1 (Fig. 1B) using an Advanced Geosciences, Inc. Supersting R8 112 passive electrode system arranged in a dipole–dipole configuration (max $n = 6$, max dipole = 12). Electrode spacing of 1-m provided high grid resolution to match the shallow, high resolution GPR data. Contact resistance for electrode takeouts was kept near or below 3 kΩ. Data was processed using Earthimager 2D (Advanced Geosciences, Inc.) with a smooth model inversion and a finite element forward model/pseudosection starting model. Negative resistivity measurements, data spikes, and misfit data points were removed (to a maximum of 10% total data points) based on histogram analysis of root mean square (RMS) error between the starting model and the inverted pseudosection. Topographic information, collected with an RTK dGPS, was added prior to inverting the profiles.

Sediment exposures were logged at the decimeter scale and included observations of unit thickness, lateral extent, nature of the lower contact, texture, clast characteristics, structure, and paleoflow measurements. Two water well records (well tag numbers 45126 and 45278 (BCME, 2011), renamed well logs (WL) A and B, respectively, in this paper; Fig. 1A) drilled in fans within the Young Lake basin were used in conjunction with sediment exposures and inferences from geophysical data to reconstruct regional stratigraphic context.

3. Results

3.1. Geomorphology and surface character of the YLER

The YLER and adjoining terraces (sub-classified as segments 1–4) extend for over 6 km in a west–east orientation, west of modern Young Lake, in the Young Lake basin (Figs. 1B and 2). Segment 1 consists of two landform elements (Fig. 2B) that extend from the western end of the ridge proper toward Rayfield River over a ridge-parallel distance of ~2.5 km. The northern landform element is in contact with bedrock on its NE flank and forms a relatively flat-topped (local relief of ~2 m), 400-m-wide terrace that is gently sloped toward segment 2. The southern landform element is an ~2-km-wide, hummocky terrace (mounds and hollows with local relief of >8 m) that is ~10 m lower in elevation than the flatter, northern landform element (947 m asl compared to 957 m asl). A bedrock knob breaks the surface of the hummocky terrace near its center. The ridge proper is composed of three segments of varying character (segments 2–4, Fig. 2). Segment 2, the westernmost section of the ridge, is ~2 km long, 85–260 m wide, and relatively flat-topped with a maximum surface elevation of 952 m asl (segment 2, Fig. 2). It is bounded to the north by enclosed, dry, sediment-floored depressions and to the south by the Bonaparte River (Fig. 2B). Slump depressions and scarps are evident along its surface and flanks. Surface material on the southern side of segment 2 is sandy gravel characterized by subrounded to rounded pebbles, cobbles, and occasional boulders (Fig. 2G). However, the north side of segment 2 is ornamented with low amplitude (0.5 m) sand dunes (Fig. 2D–F). At the eastern terminus of segment 2, the ridge surface abruptly drops in elevation to 930 m asl (adjoining segment 3). Segment 3 is an 800-m-long, round-crested ridge that narrows to <40 m wide in places and has an undulating long profile (segment 3, Fig. 2A–B). The ridge is bounded to the north by an enclosed pond-filled depression (Fig. 2B). This pond appears to be hydraulically connected to Young Lake because it shares an equivalent water surface elevation (923 m asl) and has no apparent surface outlet. The south side of segment 3 is rimmed by depressions (now incised and modified by the Bonaparte River) and scarps formed by post-depositional slumping. Segment 4 is 1.3 km long, up to 1 km wide, and relatively flat-topped (segment 4, Fig. 2A–B). The uniform flat ridge surface is broken by a large (~500-m-long) pond-filled enclosed depression that appears to be hydraulically connected to Young Lake (they have the same water surface elevation), and a gap in the ridge surface is filled by Young Lake (Fig. 2B). Several similar depressions (now modified by the Bonaparte River) form the slump rimmed southern side of the ridge. This segment gently slopes from 948 to 939 m asl toward the east, terminating 16 m above modern Young Lake (923 m asl). The first-order trend surface of all four segments of the YLER gently slopes (~3 m/km) toward modern Young Lake in the east (Fig. 2B).

3.2. YLER radar elements

High amplitude radar reflections (labeled R1–R8 in Fig. 3 and Fig. S1) traceable over multiple GPR lines were used to reconstruct the bounding surfaces of radar elements that are labeled A–L in Figs. 3 and 4 and referred to as RE-A to RE-L in the text. All radar elements are observed in GPR grid 1 except RE-J and RE-K, which are found only in grid 2 (Fig. 4). Radar elements and bounding surfaces are described in detail below.

3.2.1. RE-A

RE-A is the lowest radar element imaged and can be identified throughout the grid by rapid signal attenuation below its upper bounding surface (R1). Few 'real' reflections are visible in this element

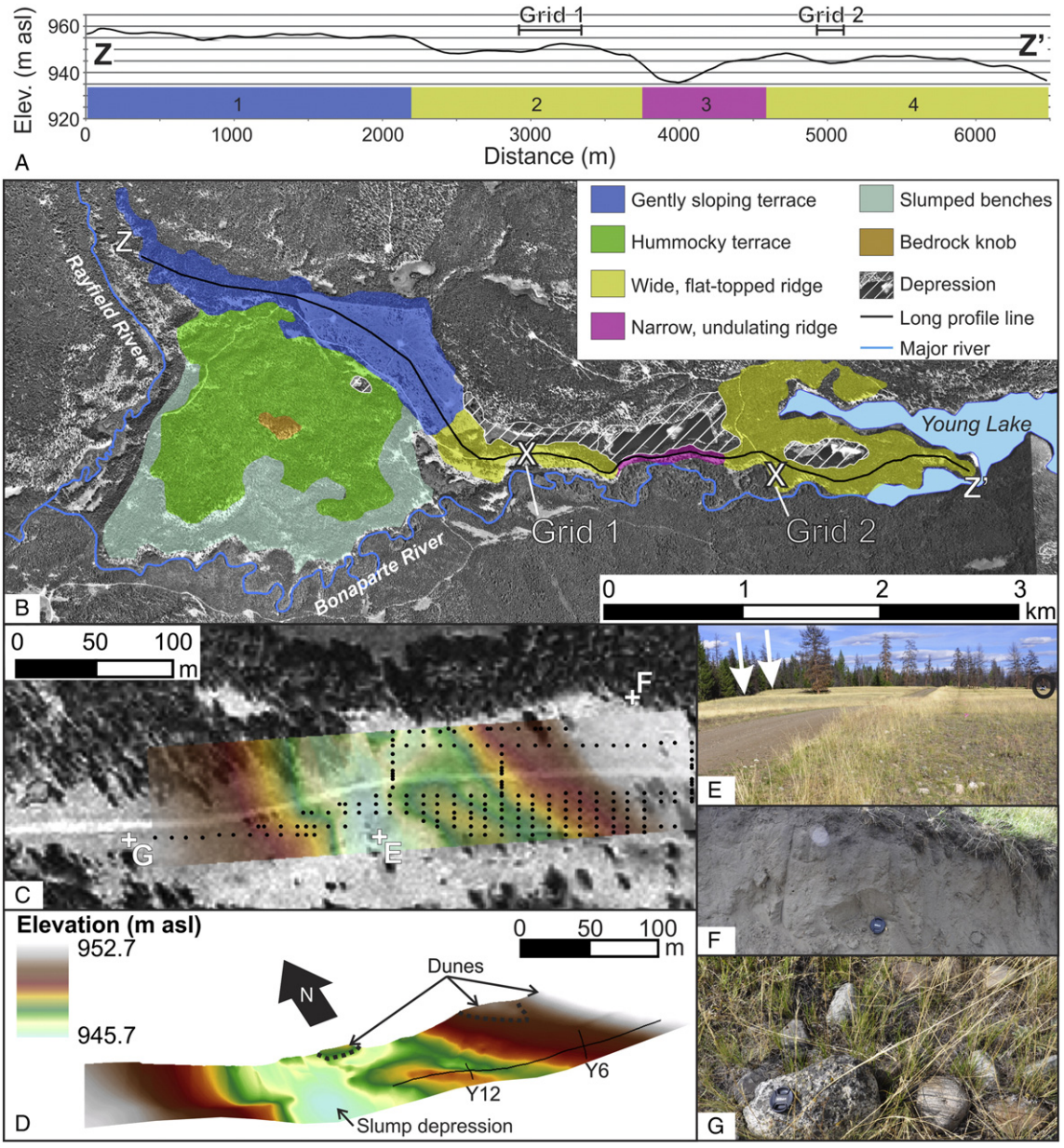

Fig. 2. (A) Topographic long profile of Young Lake esker-like ridge (8× vertical exaggeration, Geobase®, refer to B for profile path). Bars below profile correspond to legend in B, and numbers refer to landform segments discussed in the text. Linear extent of geophysical survey grids 1 and 2 are indicated by solid black lines above profile. (B) Geomorphic map of YLER and associated landforms superimposed on an orthophotograph (Province of British Columbia, 2010; refer to Fig. 1B for location) displaying geophysical survey grid locations. (C) Topography around grid 1 interpolated from RTK dGPS elevation measurements (shown as points with decimeter accuracy) along GPR lines (see elevation scale in C) superimposed on an orthophotograph (Province of British Columbia, 2010). Location of photos in E–G shown. (D) Perspective view of the DEM shown in C. Refer to text for explanation of dunes and slump. (E) Surface relief looking east along YLER at grid 1. Arrows highlight two aeolian dunes on the north side of the ridge. Truck for scale (circled). (F) Small dune exposure on the north side of segment 2. (G) Boulders, cobbles, pebbles, and sand exposed on the south side of segment 2. Camera lens cap is 6 cm in diameter.

and the lower bounding surface is not discernible. The rapid signal attenuation below R1 (Fig. 3) suggests a boundary between a highly transmissive medium (above) and a low transmissive medium (below, RE-A; Neal, 2004). R1 (940 m asl) is above modern Young Lake (923 m asl), and the Bonaparte River; therefore R1 cannot represent the water table. Till and bedrock are not observed at a depth that corresponds to R1 within WLA and WLB (Fig. 5), but a unit of silt (WLA-2) is recorded at this stratigraphic position in local water wells (Fig. 5). Therefore, RE-A is inferred to record relatively fine-grained sediments such as silt.

3.2.2. RE-B and RE-E to RE-I

RE-B (~4-m-thick) is a tabular, moderately continuous element with an irregular lower bounding surface (R1, Fig. 3) that truncates reflections within RE-A (e.g., at ~20 m on line X7, Fig. 3D). Internal reflections are planar, subparallel and onlap R1. Lines connect offset reflections crossing R2 into RE-B (dashed lines, Fig. 3) trending east and west on X3 (Fig. 3B, dip of 40 to 50°) and north on Y6 (Fig. 3C, average dip of 45°).

RE-E to RE-I are tabular in flow-parallel lines where they are at least 2–3× longer than RE-C and RE-D (Fig. 3B), resulting in a length to depth ratio that is about double that of RE-C and RE-D. They are trough-shaped in flow-perpendicular lines. RE-E to RE-I are composed of planar, subparallel reflections that onlap lower bounding surfaces (R4 to R8), although some of these planar reflections in RE-I dip slightly east. The sinuous and trough-shaped lower bounding surfaces of RE-E to RE-I are low angle (except for the lower bounding surface of RE-F (R5) that dips 22° to the west at its eastern extent in

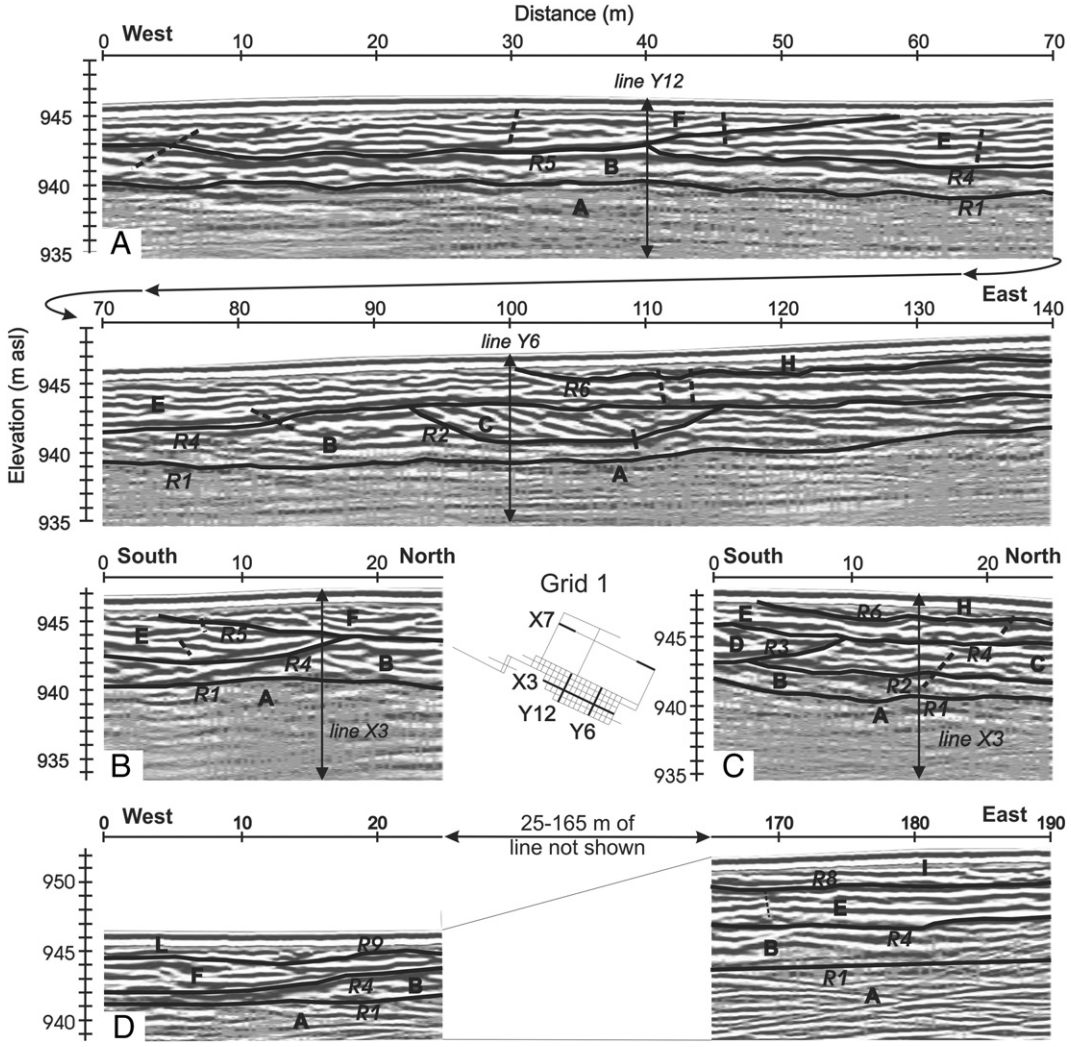

Fig. 3. Processed GPR profiles of (A) line X3, (B) line Y12, (C) line Y6, and (D) parts of line X7 from grid 1 (Figs. 1B, 2B, and C). Radar bounding surfaces (bold lines labeled R1–R9) delineate nine radar elements labeled A–F, H, I, and L (G is recorded elsewhere in line X7 (see Fig. S1); RE-J and K are recorded in grid 2, Fig. 4). The locations where GPR lines intersect are shown by labeled double-headed arrows. Dashed lines mark offset reflections. GPR profiles are shown with no vertical exaggeration.

line X3, Fig. 3A), continuously traceable across all lines, and truncate deeper reflections. The lower bounding surface of RE-I (R8) truncates RE-E (Fig. 3). Aligned offset reflections within RE-E and RE-F continue through R4 and R5, trending both east and west (Fig. 3, dips of 25 to 60°). Aligned offset reflections fully contained within RE-E to RE-G are steeper (close to 90° in some cases) and trend east and west as well as north and south in Y lines (Fig. 3).

Strong radar signal return from RE-B and RE-E through RE-I (Fig. 3) and surface observations (Fig. 2G) suggests these radar elements are composed of sand and gravel. The continuity (in both X and Y lines) and the subparallel, planar nature of reflections within RE-B and RE-E to RE-I suggest that these are plane beds (Burke et al., 2008; Rice et al., 2009) and were deposited in gravel sheets (Rice et al., 2009). Bounding surfaces R1 and R4-8 truncate lower reflections and are reactivation surfaces indicating distinct erosional events between the depositions of gravel sheets. These events may record adjustments in accommodation space in the gently sloping YLER (Wooldridge and Hickin, 2005).

3.2.3. RE-C and RE-D

RE-C and RE-D are trough-shaped elements up to 3 m thick, 25 m long (Fig. 3A), and 20 m wide (Fig. 3C). Internal reflections are downlapped onto lower bounding surfaces and exhibit an average apparent dip of 26–30° to the east in X3 and X5, and 2–3° to the south in Y6 (Fig. 3A and C). Lower bounding surfaces (R2 and R3) are continuous and truncate deeper reflections (Fig. 3). Aligned offset reflections (Fig. 3) trend east and north in X and Y lines (dip of 75° and 45° respectively), crossing from RE-C into RE-B.

The steeply dipping reflections within RE-C and RE-D (Fig. 3) are interpreted as avalanche surfaces, recording progradational slip-face deposition (Wooldridge and Hickin, 2005) at the edge of a scour into RE-B (recorded by R2 and R3, Fig. 3). Dip direction of slip-face deposits in RE-C suggest progradation, and hence formative flows, to the east, consistent with the general slope of the YLER (segments 1–4, Fig. 2A).

3.2.4. RE-J to RE-K

RE-J is one of two radar elements imaged in grid 2 (Fig. 2B) and is characterized by sets of variably dipping parallel reflections (23–30° dip toward 92° east in X5, Fig. 4A) that are undulatory to planar in cross section (Y lines, Fig. 4A). The lower boundary of RE-J is obscured by signal noise, and the upper boundary contacts the ground wave in the floor of the gravel pit (Fig. 4A). RE-K is the second radar element imaged in grid 2 (Fig. 4B) and is only visible in X7, located on an undisturbed, heavily forested area adjacent to the gravel pit and 5 m above the gravel pit floor. RE-K is composed of planar,

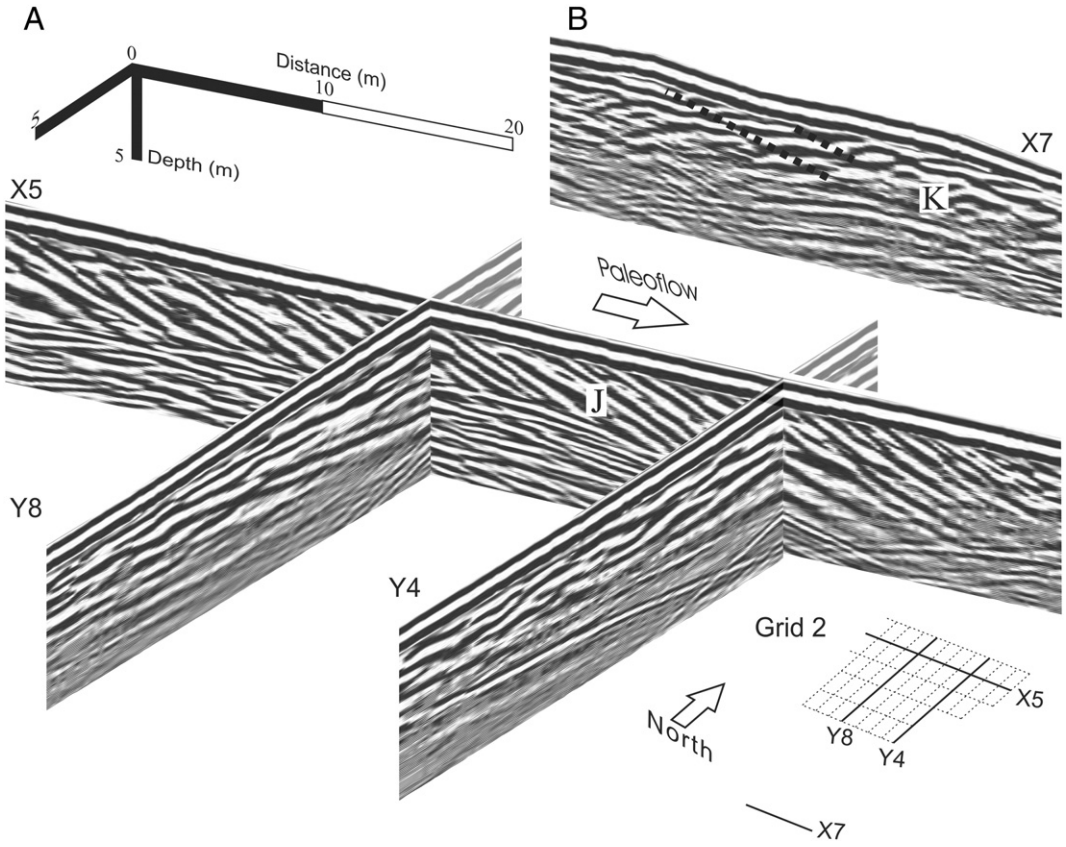

Fig. 4. (A) Fence diagram of representative processed GPR lines for grid 2 (refer to Figs. 1B and 2B for grid location) measured from the base of a partially excavated gravel pit. Relative line locations are shown by the solid lines on the grid map (bottom right). (B) Line X7 was measured on undisturbed ground 5 m above the pit floor. Dashed lines demark offset reflections. Broad diffractions at depth are caused by offline trees. GPR profiles are shown with no vertical exaggeration.

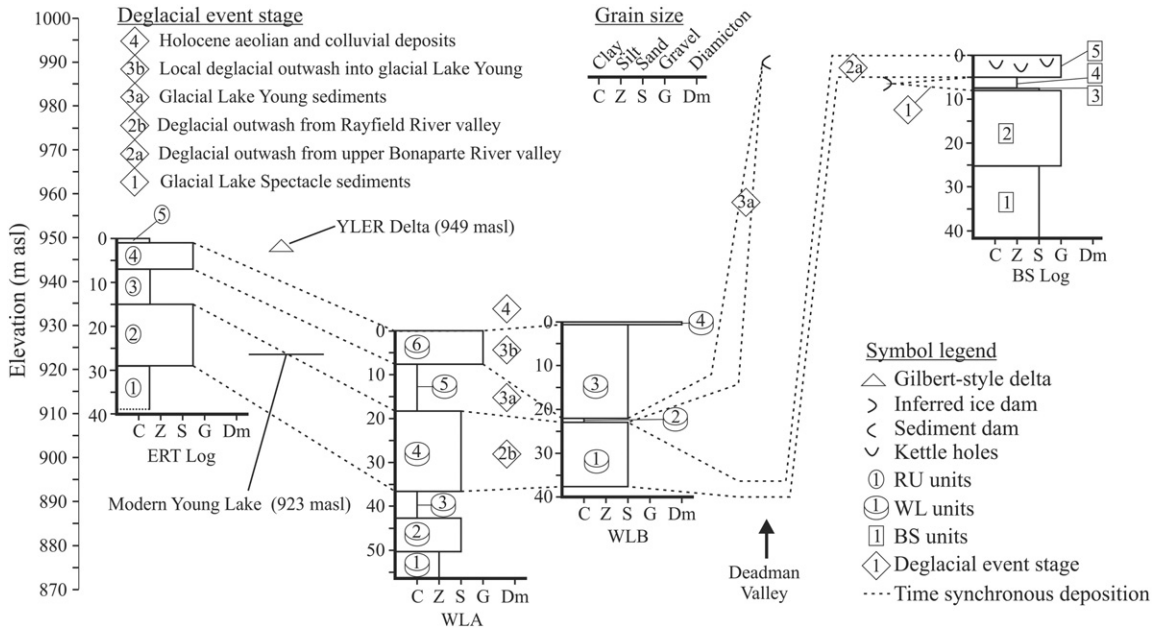

Fig. 5. Stratigraphic logs from Young Lake basin; refer to Fig. 1B for log names and locations. The electrical resistivity tomography (ERT) log is interpreted from resistivity values (RU, resistivity units) in the ERT line at grid 1 (Fig. 6). The logs are arranged in spatial order from west (ERT log) to east (BS log). For each log, the X-axis records grain size and the Y-axis indicates depth below land surface (m). Dashed lines join units interpreted to have been deposited coevally and do not necessarily represent laterally or vertically continuous deposition; erosional unconformities are not displayed. Each log records a repetitive sequence of fine (lacustrine) and coarse (outwash) sediments; diamicton is absent (except for surficial sediments of WLB). The position of Deadman Valley, the elevations of inferred ice and sediment dams (Figs. 8 and 9), the inferred delta topset/foreset boundary at grid 2 (Fig. 4) and modern Young Lake are also shown.

subparallel reflections with offset reflections that align with shallow (~2-m-deep) topographic depressions on the surface. Signal noise from trees close to the survey line prevented imaging of the contact between RE-K and RE-J. However, the spatial relationship between the lines suggests that these radar elements are stratigraphically stacked.

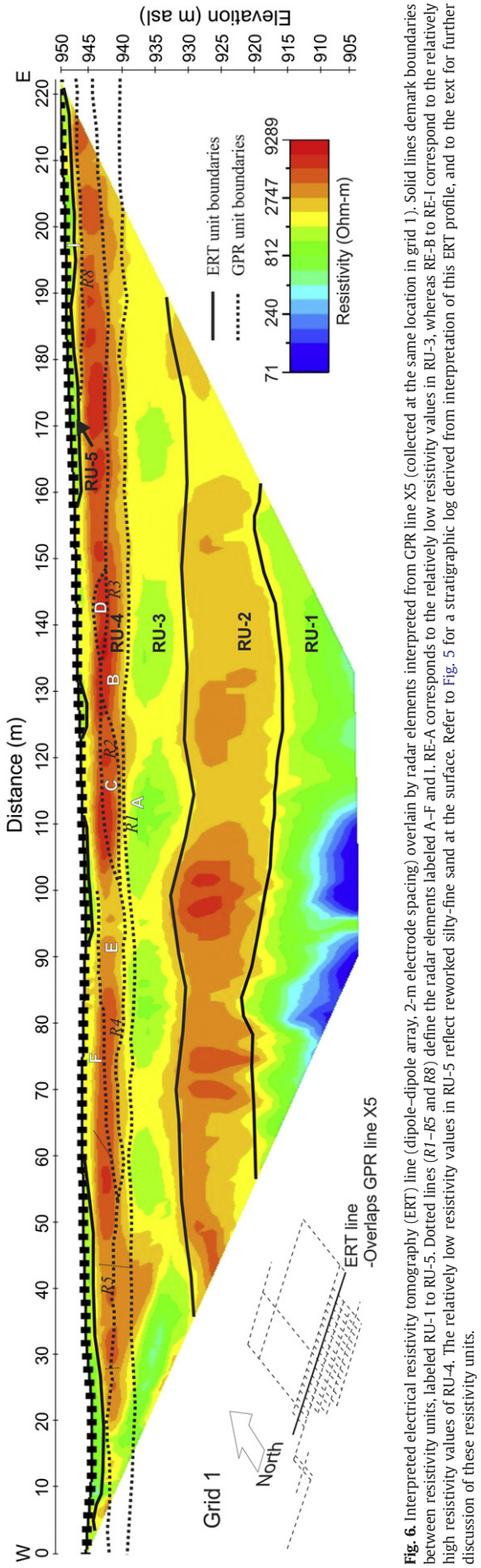

Fig. 6. Interpreted electrical resistivity tomography (ERT) line (dipole–dipole array, 2-m electrode spacing) overlain by radar elements interpreted from GPR line X5 (collected at the same location in grid 1). Solid lines demark boundaries between resistivity units, labeled RU-1 to RU-5. Dotted lines (*R1–R5* and *R8*) define the radar elements labeled A–F and I. RE-A corresponds to the relatively low resistivity values in RU-3, whereas RE-B to RE-I correspond to the relatively high resistivity values of RU-4. The relatively low resistivity values in RU-5 reflect reworked silty-fine sand at the surface. Refer to Fig. 5 for a stratigraphic log derived from interpretation of this ERT profile, and to the text for further discussion of these resistivity units.

The steeply dipping reflections of RE-J are interpreted as eastward-prograding foreset beds within a prograding, Gilbert-style delta (Postma, 1990; Jol and Smith, 1991). Foreset beds with shifting dip angles suggest slight changes in direction of lobate delta progradation (Kostic et al., 2005). The planar, subparallel reflections of X7 are interpreted as topsets (only imaged on the unmodified landform surface (X7) because 3–4 m of surface material has been removed from the gravel pit where radar grid 2 is centered). Offset reflections within X7 associated with small topographic depressions probably relate to later collapse of the delta surface, either resulting from contact and deposition overtop of melting ice blocks or settling after dewatering as lake level in the Young Lake basin fell.

3.2.5. RE-L

RE-L is thin (<2-m-thick on average), wedge-shaped and characterized by irregular reflections. These reflections are typically horizontal, but in some places dip (~20°) eastward (Fig. 3D) and downlap the lower bounding surface that is conformable with deeper reflections (Fig. 3D).

The slightly dipping reflections in this radar element suggest some vertical accretion and eastward progradation. Gullys cut through this unit expose massive, silty fine sand (Fig. 2F). Based on surficial geomorphic expression of undulatory ridges, sandy composition and planar horizontal to slightly dipping sedimentary architecture, RE-L is interpreted as recording aeolian dunes and sand sheets comparable to those observed nearby on the Fraser Plateau by Lian and Huntley (1999) and Plouffe (2009).

3.3. YLER resistivity units

The ERT line had a maximum depth of penetration of ~48 m below the surface of the YLER. Five resistivity units are identified and hereafter labeled RU-1 to RU-5 (Figs. 5 and 6). For the descriptions below, we group RU-1, 3, and 5, and RU-2 and 4 because they have similar resistivity characteristics (Figs. 5 and 6). Undulating boundaries at unit contacts are probably the result of signal noise within the data set (Kilner et al., 2005).

3.3.1. RU-1, RU-3, and RU-5

RU-1 (≥10-m-thick, no lower contact observed) and RU-3 (~8-m-thick) average ~850 Ωm (Fig. 6). However, RU-1 displays a gradient from higher resistivity values close to RU-2 toward lower resistivity values at depth. RU-5 is an irregular unit (~1-m-thick) that contacts the surface of the YLER in places and has a relatively low average resistivity (~800 Ωm).

RU-1, 3, and 5 display resistivity values within the range of fine-grained sediments such as sandy-silt and diamicton (Palacky, 1987; Reynolds, 1997). The stratigraphic position of RU-3 directly corresponds to RE-A, interpreted as silt in GPR grid 1 (Fig. 3). The rapid GPR signal attenuation within RE-A (Fig. 3) is consistent with the low resistivity values measured in the ERT lines. Furthermore, at the landform surface and in gully walls along the north side of YLER segment 2 (Fig. 2F), an ~1-m-thick unit of silty fine sand corresponds to the low resistivity RU-5. Consequently, RU-1, 3, and 5 probably record fine material such as silty fine sand or silt. The gradation to lower resistivity values with depth in RU-1 (~922 m asl) is attributed to low resistance approaching the water table (Bonaparte River level is 920 m asl, and lakes in enclosed depressions to the north are at 923 m asl).

3.3.2. RU-2 and RU-4

RU-2 (~14-m-thick) averages ~3000 Ωm (can be as high as 6000 Ωm), whereas RU-4 (~6-m-thick) averages ~5000 Ωm (can be as high as 8100 Ωm). These relatively high resistivity values suggest that RU-2 and RU-4 record gravel and/or sand (Palacky, 1987). This is consistent with the presence of cobbles, pebbles, and sand on the

Fig. 7. Sediments of the Bonaparte section (BS, Fig. 1B). (A) Bonaparte section exposure showing unit (BS-1 to BS-5) boundaries. Refer to text for unit descriptions. (B) Close-up of putative deglacial units within the Bonaparte section, including finely laminated sediments of BS-4 and coarse gravel of BS-5.

surface of the YLER, where RU-4 extends to the landform surface (Figs. 2G and 6), and with the good electromagnetic signal penetration through RE-B to RE-I in GPR grid 1 (correlative with RU-4; Fig. 6). RU-2 has similar resistivity values, and nearby water well records also record sand and gravel in similar stratigraphic positions to RU-2 and RU-4 (Fig. 5). We therefore interpret these resistivity units as sand and gravel.

3.4. The Bonaparte section

The Bonaparte section is a 41-m-thick, valley-side exposure consisting of five stratigraphic units (BS-1 to 5, Figs. 5 and 7A–B) exposed in a river cut 10 km upflow from the YLER, along the upper Bonaparte River (BS, Fig. 1B). The lowest unit (BS-1, Fig. 7A) is at least 6.4-m-thick. Beds of 0.5-m-thick moderately consolidated, well-sorted, planar, cross-bedded medium sand alternate with 1-m-thick cosets of type B cross lamination (15 mm crest height, 35° angle of climb) and occasionally type A cross lamination that record paleoflow toward the SW. Based on texture and structure, BS-1 was deposited in a subaqueous environment, likely lacustrine, with SW flowing turbidity currents (Lowe, 1982).

BS-2 is a 17.2-m-thick, upward-fining unit of subrounded to rounded, clast-supported cobble to boulder gravel in a sparse matrix of coarse sand to granule (Fig. 7B) with a sharp lower contact. The unit includes 0.5-m-thick lenses of planar-bedded medium sand. The sharp lower contact indicates partial erosion of BS-1 prior to deposition of BS-2. Given clast size, roundness, and framework support, the unit was likely deposited in a high energy fluvial environment.

BS-3 is a 0.5-m-thick unit of massive, coarse sand containing isolated angular to subrounded pebbles concentrated within the lower half of the unit (Fig. 7B) and has a sharp lower contact. The large proportion of massive sand combined with isolated pebbles suggests deposition in a hyperconcentrated flow (Postma et al., 1988), possibly into a lake (see BS-4 below). The large, rounded clasts of BS-2—contrasted with the small, angular clasts in BS-3—suggest the hyperconcentrated flow was not powerful enough to erode or incorporate much of BS-2. Yet the sharp lower contact of BS-3 is an unconformity, probably reflecting erosion from another (earlier) agent of which BS-3 was the waning stage or which BS-3 directly followed.

BS-4 is a 2.5-m-thick unit of horizontally-laminated fine sand and silt with three beds of massive, medium sand up to 5 cm in thickness (Fig. 7B). These beds dip 10° toward the Bonaparte River, and the unit has a sharp lower contact. The horizontally-laminated fine sand and silt is characteristic of suspension settling in a slackwater environment such as a lake (Ashley, 1975; minimum elevation of lake surface 984 m asl based on the maximum elevation of BS-4). The beds of massive medium sand likely record episodic turbidity flows (Lowe, 1982) across the lake bottom.

BS-5 spans the upper 5 m of the exposure and contains moderately sorted, weakly upward-fining, mainly clast-supported cobble gravel with a coarse sand to granule matrix (Fig. 7B). Clasts are rounded to well-rounded, and some display worn glacigenic wear features (Krüger, 1984). The surface of the unit is gently sloped toward the Bonaparte River and is pocked by circular depressions up to 3 m deep. The well-rounded clasts and moderate sorting of BS-5 suggest deposition in a moderately energetic fluvial environment. The upward-fining trend suggests an overall decrease in energy within the fluvial system, perhaps as a result of channel migration away from deposition at the exposure location. The worn glacigenic wear features suggest the clasts are reworked glacigenic material. The circular depressions on the surface are interpreted as kettle holes related to the melt-out of buried ice (cf. Maizels, 1992; Fay, 2002).

3.5. Geomorphic evolution and drainage reversal of Deadman Valley

The upper Deadman Valley has been recently classified as a large meltwater channel (Huscroft, 2009), but no paleoflow direction has been attributed to it. Today, an unnamed creek drains upper Deadman Valley northward to Young Lake. However, a raised channel and erosional remnants elevated 35 m above the modern floor of Deadman Valley (Fig. 8) suggest that this drainage may have been reversed in the late glacial period, linking it to the upper Bonaparte River valley and the Bonaparte section. Therefore, when it was an active meltwater channel, the Deadman Valley may have supported southward drainage contiguous from the upper Bonaparte River valley. A 2.3-m/km southward-dipping slope connects the top of BS-5 (991 m asl; Figs. 5 and 8C) with the upper surface of the erosional remnants and the floor of the raised channel (~984 m asl; RC, Fig. 8C). This slope is consistent with proglacial outwash streams elsewhere (Maizels, 1979; Chew and Ashmore, 2001), and therefore BS-5 likely records progacial floodplain deposition by the late glacial/early Holocene Bonaparte River (paleo-Bonaparte River terrace) prior to its incision to modern level (950 m asl). The two erosional remnants

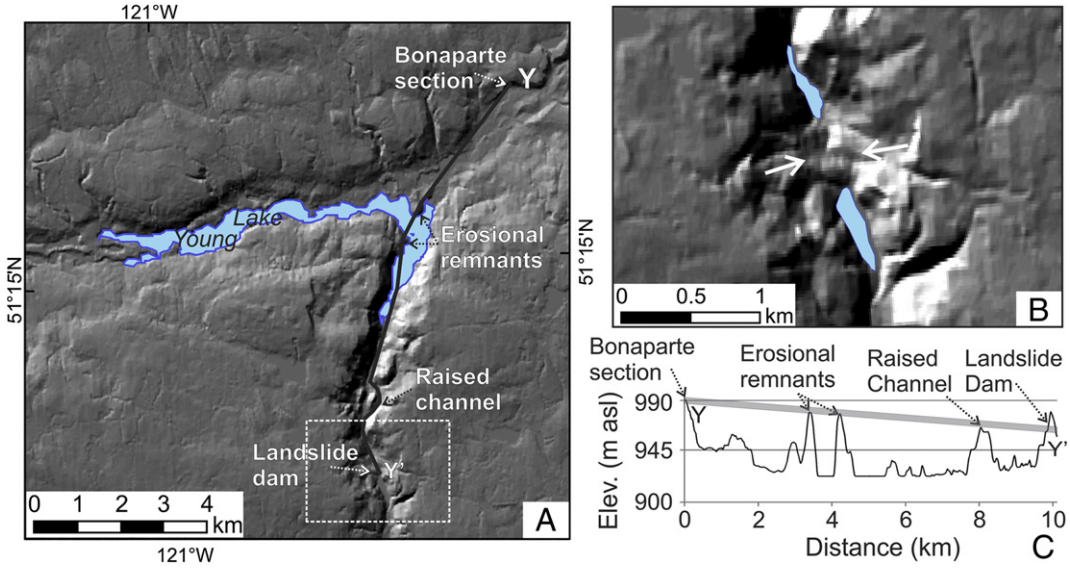

Fig. 8. (A) Terrain hillshade (Geobase®) showing Young Lake basin and location of a topographic profile starting in upper Bonaparte River valley (Y) and terminating in Deadman Valley (Y′). Dashed box indicates location of B. (B) White arrows highlight movement direction of coalescent slump blocks that impounded Deadman Valley during deglaciation (deglacial event stage 3a, Figs. 5 and 9D) and now form a drainage divide along modern Deadman Valley. (C) Topographic profile from Y to Y′. Vertical exaggeration is 30×. The gray bar shows an inferred regional gradient of 2.3 m/km for the paleo upper Bonaparte–Deadman Valley drainage system (deglacial event stage 2A and B, Figs. 5 and 9A and B) connecting (from Y to Y′) the top of unit BS-5 (Fig. 5), the upper surface of the erosional remnants and the base of the raised channel. It intersects with the landslide dam (Y′) responsible for reversing flow in Deadman Valley. Bar width accounts for vertical error in the DEM.

(ER, ~985 m asl, Fig. 8C) adjacent to Young Lake are composed of ice-contact sediments and hummocky till (cf. Bednarski, 2009) and are just slightly higher than the floor of the raised channel (RC, Fig. 8C). These erosional remnants were probably part of the paleo-Bonaparte drainage through Deadman Valley and were partially eroded as the river incised through Deadman Valley fill.

The bathymetry of Young Lake displays a series of closed depressions below the water surface, from 20 to 60 m deep (Balkwill, 1980). These depressions likely record the positions of ice blocks within the Young Lake basin that blocked the westward flow of water, forcing drainage of the paleo-Bonaparte River south through Deadman Valley. Furthermore, many of the fans deposited by streams draining into the Young Lake basin are pocked by circular depressions resembling kettle holes. This suggests that the position of modern Young Lake was probably occupied by stagnating, inactive ice following active ice retreat from the Young Lake basin. A long, low drainage divide in the valley 3.4 km south of Young Lake is formed from several coalescent slump blocks from the walls of Deadman Valley (Huscroft, 2009). This earthen dam likely terminated southerly drainage of the paleo-Bonaparte River through Deadman Valley.

4. Discussion

4.1. Stratigraphic correlations within Young Lake basin

The sediments located in the Bonaparte section, well logs A and B, and inferred from geophysical investigations along the YLER can be correlated across Young Lake basin (Fig. 5). The stratigraphically lowest and therefore oldest sediments exposed in Young Lake basin are recorded by BS-1 and BS-2, RU-1 and WLA-1, 2, and 3 (Fig. 5). No correlation is attempted for these units as they likely represent deposition prior to the deglacial period. Rather, we focus on time-stratigraphic correlation based on stratigraphic position, elevation, composition, and environmental interpretation for the upper units in the basin fill that are likely deglacial in age. Units are grouped into four deglacial event stages (DES, Fig. 9).

The fine-grained units at YLER (RU-1, RU-3, and RE-A, Figs. 3, 5, and 6) and in the well logs in Young Lake basin (WLA-3, WLA-5, and WLB-2, Fig. 5) are too low in elevation to correlate with the lake sediments of BS-3 and BS-4; and no lake sediments or landforms are found in the rest of Young Lake basin at elevations similar to those in the BS. Therefore, ice must have been present everywhere in Young Lake basin, except the upper Bonaparte River valley, in order to prevent expansion of this lake (herein named glacial Lake Spectacle) and more widespread deposition. This represents the first stage in the deglacial event sequence within Young Lake basin (DES-1, Figs. 5 and 9A).

Coarse-grained unit BS-5 is inferred to correlate with units RU-2, WLA-4, and WLB-1 (Fig. 5) based on grain size and stratigraphic position. The sediments, which are consistent with deposition in a proglacial outwash system, are in line with confluent southward flow of the paleo-upper Bonaparte River and paleo-Rayfield River out of Young Lake basin through Deadman Valley. RU-2, WLA-4, and WLB-1 connect flow out of the paleo-Rayfield River with Deadman Valley. These units likely record later stage floodplain deposition from paleo-Rayfield River atop of and amongst dead ice where modern Young Lake and the YLER now exist, after the active ice front had retreated from Young Lake basin (Figs. 5 and 9C, DES-2a–b).

In the western arm of Young Lake basin, units RU-3, WLA-5, and WLB-2 all record fine-grained sedimentation into a high stage lake up to at least 986 m asl (herein named glacial Lake Young, Figs. 5 and 9D) in Young Lake basin (Figs. 5 and 9D, DES-3a). This lake formed because the southern outlet of the Rayfield–Bonaparte drainage system through Deadman Valley was blocked by slumped material (Fig. 8), likely caused by debuttressing as a result of deglaciation and slope undercutting by earlier meltwater flow through Deadman Valley. The modern route of Bonaparte River through the lower Bonaparte River valley to the west is inferred to have been blocked by ice (Fig. 9D).

Coarse-grained, deltaic units within YLER (RU-4 including RE-B to RE-K) cap the glaciolacustrine sequence locally (Figs. 3, 5, and 6). WLA-6 and WLB-3 are interpreted to be deposited coevally with RU-4 because of their similar coarse-grained character and stratigraphic position directly atop finer-grained units below but above the elevation of modern Young Lake (Fig. 5). The coarse-grained character of sediments in WLA-6 and WLB-3 is consistent with deposition in fluvially-dominated alluvial fans (e.g., Ryder, 1971; Ballantyne, 2002) or low energy subaqueous fans (Lowe, 1982; Winsemann et al., 2007), suggesting that WLA and WLB were drilled into

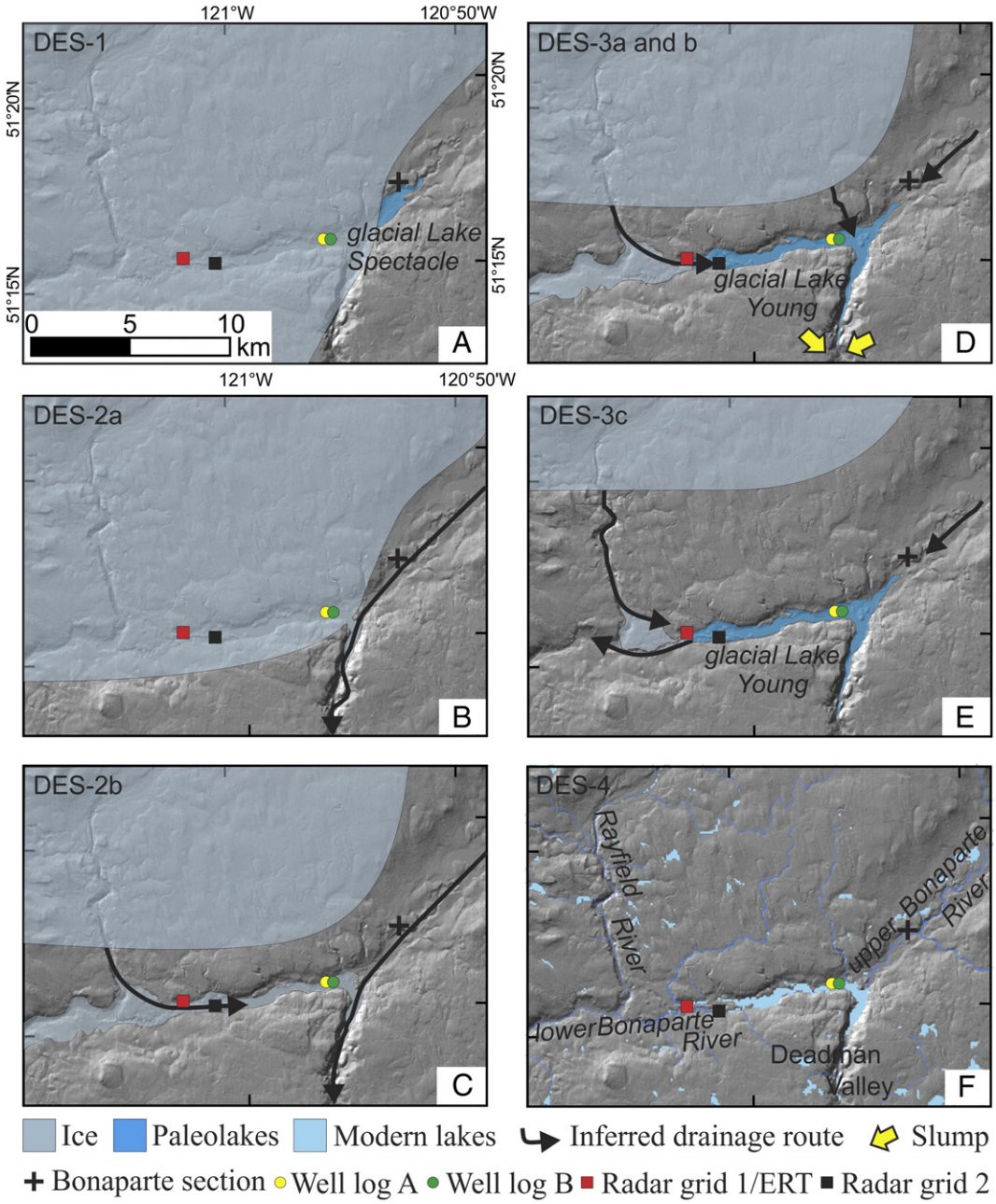

Fig. 9. Geomorphic evolution of the Young Lake basin during CIS retreat. (A) Deglacial event stage (DES) 1: The ice margin is downwasting and backwasting to the NW, opening the upper Bonaparte River valley, forming glacial Lake Spectacle (gLS), and resulting in the deposition of glacial lake sediments (BS-3 and BS-4, Figs. 5 and 7B). (B) DES-2a: The ice margin retreats further, allowing drainage from the paleo-upper Bonaparte River south through Deadman Valley, resulting in deposition of river terrace gravel (BS-5, Figs. 5 and 7B–C) and the sediments within the erosional remnants (Fig. 8A), and incision of the Deadman Valley raised channel (RC, Fig. 8A). (C) DES-2b: Ice retreat opens up the Rayfield River valley, but downwasting ice blocks the lower Bonaparte River valley resulting in drainage east into Young Lake basin overtop of stagnating ice (recorded by RU-2, Figs. 5 and 6; WLA-4, WLB-1, Fig. 5) and south down Deadman Valley (raised channel from DES-2a is abandoned after further glaciofluvial erosion of Deadman Valley). This is the first stage in the formation of YLER. (D) DES-3a: Coalescent slumps (Fig. 8) into Deadman Valley dam this drainage route forming glacial Lake Young (gLY) and resulting in the deposition of glaciolacustrine sediments (recorded by RE-A, Figs. 3 and 5; RU-3, Figs. 5 and 6; WLA-5 and WLB-2, Fig. 5). DES-3b: Evolution of a Hjulstrom-style delta occurs as sediment progrades eastward over lake bottom sediments and amongst wasting ice blocks in the lower Bonaparte River valley at GPR grid 1 (recorded by RE-B to RE-I, Fig. 3; and RU-4, Figs. 5 and 6). A Gilbert-style delta progrades eastward over lake bottom sediments at GPR grid 2 (recorded by RE-J and K, Fig. 4), as inflows encounter deeper lake water. At this time (or perhaps slightly later) meltwater drainage from the plateau surface to the north deposits outwash sediments in valley marginal fans within the Young Lake basin (recorded by WLA-6 and WLB-3, Fig. 5); (E) DES-3c: Lake level rises, overtops the ice dam in the lower Bonaparte Valley (the lowest possible outlet at the west end of Young Lake), and rapidly drains, establishing the path for modern Bonaparte River drainage. (F) DES-4: All dead ice has melted out and the modern lower Bonaparte River drains west from modern Young Lake. Rayfield River no longer drains into Young Lake basin and south through Deadman Valley, but has cut through the ice contact sediments at the west end of the YLER and joined the westward-flowing lower Bonaparte River. Ice margin locations are schematic in C–E.

valley-side, kettled fan sediments. The fans are connected north to the plateau surface by long, deeply incised channels with small modern catchments. Consequently, the fans were likely built by sediment deposited by proglacial outwash streams (DES-2b to 3b, Fig. 9C and D). Kettles holes suggest that fan sedimentation occurred atop stagnating ice in the Young Lake basin, an inference consistent with that made for RU-4 of the YLER. As ice retreat on the plateau progressed, these meltwater channels were ultimately abandoned.

RU-5 (including RE-L, Figs. 3, 5 and 6) and WLB-4 cap their respective stratigraphic sequences and, although disparate in sedimentology, record local postglacial processes (Figs. 5 and 9F, DES-4). The fine-grained sediments of RU-5 (Fig. 6) record postglacial aeolian activity; whereas the thin, coarser-grained diamicton of WLB-4 records colluvial activity.

4.2. Genesis of the Young Lake esker-like ridge

Two hypotheses have been proposed for the genesis of the YLER: (i) it is an esker formed in an ice-walled channel with meltwater flows from east to west (Tipper, 1971c); and (ii) it is an ice-contact, poorly-sorted, stratified deposit aggraded by meltwater flowing from east to west (Plouffe, 2009). New mapping shows that the landform has a general slope to the east with varied morphology (Fig. 2). It is composed of coarse outwash material (RU-2, Figs. 5 and 6) overlain by sandy silt or silty lacustrine sediments (RE-A and RU-3, Figs. 3, 5, and 6; cf. Pellicer and Gibson, 2011) typical of the distal end of a deltaic environment (Smith and Ashley, 1985), topped by gravelly deltaic sediments (RE-B to RE-K, RU-4, Figs. 3–6) recording delta progradation and flow from west to east atop and amongst dead ice.

Tabular gravel sheets and scour fills are characteristic of subaerial braided stream floodplains (Heinz and Aigner, 2003; Sambrook Smith et al., 2006) and Hjulstrom-style deltas fed by proglacial rivers (Church and Gilbert, 1975; Postma, 1990; Jol and Smith, 1991) rather than subglacial esker fills. Subglacial esker fills deposited by flow under hydrostatic pressure are typically characterized by deposition in large convex-up bedforms and macroforms (e.g., Brennand, 1994; Burke et al., 2008). Therefore, the YLER is not a classic subglacial esker (cf. Brennand, 2000). The low relief, gently-sloping character of the terrace that forms the northern landform element of segment 1 is attributed to deposition by an outwash stream directly on land. The flat-topped character of segment 2 (Fig. 2A and B), along with its largely undisturbed primary bedding and minor amounts of faulting with consistent dips toward the landform flanks (corresponding to slump scarps at the landform surface), suggest that deposition in segment 2 was also mainly on land rather than ice. Conversely, if the landform had been deposited on top of ice, we would expect highly disturbed primary bedding and more extensive, irregularly oriented faults. The presence of distinct fault scarps and kettle holes on the north side of the ridge at segment 2 suggests that it was deposited atop of and in contact with dead ice and that its flanks partially collapsed after melting of this ice support (Maizels, 1992; Fay, 2002). By extension, we attribute the hummocky landform element of segment 1, undulatory character of segment 3, and the pond-filled depressions north of segment 3 and within segment 4 (Fig. 2B) to sedimentation atop of and in contact with dead ice. The surface of YLER is ornamented by postglacial aeolian sand sheets and dunes (RE-L and RU-5, Figs. 3 and 6), recording Holocene reworking and sedimentation.

In summary, the YLER formed as ice-marginal glaciolacustrine sediments and braided outwash/deltaic sediments were deposited on top of decaying ice and/or within an ice-walled canyon in decaying ice. Consequently, the YLER is an ice-contact deposit (Plouffe, 2009) that is best classified as a composite landform composed of a kame terrace (northern landform element of segment 1), deltas and kames that include elements of deposition atop ice (segment 4 and southern landform element of segment 1), and an esker deposited on top of and/or containing buried ice within a subaerial ice-walled canyon (segments 2 and 3). The Hjulstrom-style and Gilbert-style deltas (RE-B to RE-K, Figs. 3 and 5; RU-4, Fig. 6) were deposited by a stream flowing east from Rayfield River valley (Figs. 2B and 9C–E).

4.3. Deglacial and early Holocene evolution of Young Lake basin

Reconstruction of the evolutionary history of Young Lake basin must accommodate regional geomorphology and stratigraphy of the basin and eastward paleoflow directions recorded by the YLER. The valleys that are confluent on Young Lake basin (Deadman Valley, Rayfield River valley and upper Bonaparte River valley) are antecedent pre-glacial valleys (Andrews et al., 2011; Plouffe et al., 2011) that were deepened during the last glacial period by the erosion of meltwater channeled from the Fraser Plateau surface and the decaying CIS margin (DES-1 to 4, Fig. 9).

As ice began to decay over Young Lake basin, the first event (DES-1) recorded in the basin fill was the formation of the small, ice-dammed glacial Lake Spectacle within the upper Bonaparte River valley, marked by the deposition of BS-3 and BS-4 (Figs. 5 and 7B, DES-1, Fig. 9B).

Broad regional ice retreat NW toward the ice divide over the Coast Mountains (Tipper, 1971a) would have caused ice retreat away from the entrance to Deadman Valley opening an outlet (south through Deadman Valley) through which glacial Lake Spectacle was able to drain. Ice in the west arm of Young Lake basin blocked the modern lower Bonaparte River valley forcing the paleo-upper Bonaparte River to also flow south through Deadman Valley (DES-2a, Fig. 9B). During this period, the raised channel in Deadman Valley (RC, Fig. 8A) was incised and a river floodplain aggraded. The latter is recorded in the sediments within the erosional remnants along Deadman Valley (ER, Fig. 8A) and the gravel in BS-5 (Figs. 5 and 7B). With further ice retreat, downwasting continued within Young Lake basin, resulting in detachment of dead ice blocks from the main backwasting ice margin. Formation of the YLER was first characterized by deposition of gravel and sand in an outwash stream flowing east overtop and between this stagnating ice along the lower Bonaparte River valley (RU-2, Figs. 5 and 6; WLA-4 and WLB-1, Fig. 5) through the area occupied by modern Young Lake before joining the paleo-upper Bonaparte River as it flowed south through Deadman Valley (DES-2b, Fig. 9C).

Opposing slump block failures in Deadman Valley (Fig. 8B) formed an earthen dam at what is now a drainage divide along Deadman Valley, ponding glacial Lake Young in Young Lake basin to an elevation of ~949 m asl (maximum elevation of Gilbert-style delta foreset/topset boundary; DES-3a and b, Fig. 9D), and allowing the accumulation of fine-grained lake bottom sediments (RE-A, Fig. 3; RU-3, Figs. 5 and 6; WLA-5 and WLB-2, Fig. 5). During this phase, an outwash stream was still delivering sediment from the Rayfield River valley through an unroofed, ice-walled channel (within the dead ice) into glacial Lake Young. This resulted in the deposition of a shallow water, Hjulstrom-style delta (RE-B to RE-I, Fig. 3) within the ice walls where lake depth was low and, following progradation, a Gilbert-style delta (Fig. 4; YLER delta, Fig. 5) where lake depth increased near the dead ice margin in Young Lake basin (DES-3a and b, Fig. 9D). Also at this time, meltwater channels were still delivering sediments from the northern plateau surface to valley marginal fans overtop of stagnating ice in the Young Lake basin (WLA-6, WLB-3, Fig. 5).

With the rising water level in glacial Lake Young and decaying ice in the Bonaparte Valley, a natural spillway developed to the west over the lowest point in the downwasting ice. This spillway was proximal to the southern boundary of the YLER and generally followed the course of the modern lower Bonaparte River (DES-3c, Fig. 9E). Water flow through the lake spillway enhanced outlet incision through the ice dam (via thermomechanical melting of the underlying ice) and facilitated rapid lake drainage, releasing up to 0.145 km^3 of water down the Bonaparte Valley.

Following lake drainage, deltaic and lake-bottom sedimentation ceased and the modern outlet for Young Lake through the lower Bonaparte River valley was established (DES-4, Fig. 9F). The Rayfield River also responded to the new base level by incising through segment 1 of YLER (Fig. 2B) to establish its modern confluence with the Bonaparte River west of Young Lake. Subsequent loss of lateral and buried ice support through melting led to exposure of the YLER,

localized slope failure, and kettle hole development. Immediately following deglaciation, and prior to stabilization by vegetation, aeolian (Fig. 2D–F; RE-L, Fig. 3; RU-5, Fig. 6) and colluvial sedimentation (WLB-4, Fig. 5) were active on the surface of the YLER and within the broader Young Lake basin.

In summary, geomorphic inversion of YLER based on detailed morpho-sedimentary knowledge at the landform scale and basin-scale geomorphic and stratigraphic insight suggests northwestward ice-marginal retreat. This is in contrast to existing interpretations relying on reconnaissance level geomorphology which favor eastward retreat (Tipper, 1971c; Plouffe et al., 2011), but is consistent with the regional pattern of CIS retreat from SE to NW across the southern interior plateaus inferred from the glacioisostatic tilt of proglacial lake water planes to the south (Fulton and Walcott, 1975; Johnsen and Brennand, 2004).

5. Implications for robust geomorphic inversion

Through detailed morpho-sedimentary and basin analysis we have shown that YLER is an ice-contact meltwater deposit (Plouffe, 2009) that is best classified as a composite landform composed of a kame terrace, kames, delta, and esker deposited by a westward flowing outwash stream through and around dead ice. This insight supports northwestward ice-marginal retreat across Young Lake basin, in contrast to the eastward retreat implied by existing interpretations based largely on rudimentary mapping (Tipper, 1971b; Bednarski, 2009; Plouffe et al., 2011).

Our data confirm that eskers do not always form in subglacial R-channels (cf. Shreve, 1985; Boulton et al., 2009), and so the presence of an esker alone cannot be used to make generic inferences concerning deglacial patterns and subglacial hydrology (Owen, 1997). Esker formation in Young Lake basin took place within an unroofed, ice-walled channel and included supraglacial, subaerial, and subaqueous deposition. Such esker formation must have been supplied by water produced from sources in addition to basal melting that is often assumed to be the primary water supply in numerical models used to explain esker patterns and infer ice dynamics (Boulton et al., 2007; Hooke and Fastook, 2007). Only if the morpho-sedimentary relationships in eskers support deposition in subglacial ice tunnels should eskers be interpreted as such in paleoglaciological reconstructions based on geomorphic inversion.

This study demonstrates that the accuracy of paleo-ice sheet reconstructions is often compromised when such reconstructions are derived from geomorphic inversions that rely primarily on rudimentary landform identification and geomorphic context, and assumptions about landform genesis (e.g., Kleman and Borgstrom, 1996). Rather, we argue that accurate paleo-ice sheet reconstructions require integrated knowledge of basin-scale geomorphic and stratigraphic context, and of landform-scale morpho-sedimentary relationships. In field areas with relatively poor sedimentary exposures the application of multiple shallow geophysical tools may be pivotal to developing an understanding of subsurface sedimentary architecture, allowing for robust paleo-ice sheet reconstructions.

Supplementary data to this article can be found online at http://dx.doi.org/10.1016/j.geomorph.2013.02.005.

Acknowledgments

This work was supported by a GSA Student Research Grant to AJP, an NSERC Discovery Grant and Research Tools and Instruments Grants to TAB, and a scholarship to MJB from The Leverhulme Trust. We are grateful to John Woodward and Northumbria University for loan of the GPR and to Alain Plouffe for the loan of aerial photographs and helpful conversations about the field area. We thank Jared Peters, Dave Sacco, and Tyler Williams for assistance in the field.

References

Andrews, G.D.M., Russell, J.K., 2008. Cover thickness across the Southern Interior Plateau, British Columbia (NTS 092O, P; 093A, B, C, F): constraints from water-well records. Report 2008-1, Geoscience BC, Vancouver BC, pp. 11–20.
Andrews, G.D.M., Plouffe, A., Ferbey, T., Russell, J.K., Brown, S.R., Anderson, R.G., 2011. Bedrock elevation and the thickness of Neogene and Quaternary cover across the Interior Plateaus, Intermontane Belt, British Columbia: analysis of water-well drill records and implications for exploration potential. Canadian Journal of Earth Sciences 48 (6), 973–986.
Ashley, G.M., 1975. Rhythmic sedimentation in glacial Lake Hitchcock, Massachusetts–Connecticut. In: Jopling, A.G., MacDonald, B.C. (Eds.), Special Publication, 23. Society of Economic Paleontologists and Mineralogists, Tulsa, OK, pp. 304–320.
Balkwill, J.A., 1980. Young Lake. Resource Analysis Branch, British Columbia Ministry of the Environment, Biological Systems Section, scale 1:6000, Victoria.
Ballantyne, C.K., 2002. Paraglacial geomorphology. Quaternary Science Reviews 21, 1935–2017.
Banerjee, I., Mcdonald, B.C., 1975. Nature of esker sedimentation. In: Jopling, A.G., MacDonald, B.C. (Eds.), Special Publication, 23. Society of Economic Paleontologists and Mineralogists, Tulsa, OK, pp. 132–154.
Bednarski, J.M., 2009. Surficial Geology, Bridge Lake, British Columbia. Open file 5839, Geological Survey of Canada, scale 1:50000, Ottawa, ON.
Bevier, M.L., 1983. Regional stratigraphy and age of Chilcotin Group basalts, south-central British Columbia. Canadian Journal of Earth Sciences 20, 515–524.
Boulton, G.S., Lunn, R., Vidstrand, P., Zatsepin, S., 2007. Subglacial drainage by groundwater-channel coupling, and the origin of esker systems: part II—theory and simulation of a modern system. Quaternary Science Reviews 26, 1091–1105.
Boulton, G.S., Hagdorn, M., Maillot, P.B., Zatsepin, S., 2009. Drainage beneath ice sheets: groundwater-channel coupling, and the origin of esker systems from former ice sheets. Quaternary Science Reviews 28, 621–638.
Brennand, T.A., 1994. Macroforms, large bedforms and rhythmic sedimentary sequences in subglacial eskers, south-central Ontario: implications for esker genesis and meltwater regime. Sedimentary Geology 91, 9–55.
Brennand, T.A., 2000. Deglacial meltwater drainage and glaciodynamics: inferences from Laurentide eskers, Canada. Geomorphology 32, 263–293.
British Columbia Ministry of Environment (BCME), 2011. WELLS ground water wells database. http://www.env.gov.bc.ca/wsd/data_Searches/wells/index.html (Accessed May 2011).
Burke, M.J., Woodward, J., Russell, A.J., Fleisher, P.J., Bailey, P.K., 2008. Controls on the sedimentary architecture of a single event englacial esker: Skeiðarárjökull, Iceland. Quaternary Science Reviews 27, 1829–1847.
Burke, M.J., Brennand, T.A., Perkins, A.J., 2012. Transient subglacial hydrology of a thin ice sheet: insights from the Chasm esker, British Columbia, Canada. Quaternary Science Reviews 58, 30–55.
Chew, L.C., Ashmore, P.E., 2001. Channel adjustment and a test of rational regime theory in a proglacial braided stream. Geomorphology 37, 43–63.
Church, M., Gilbert, R., 1975. Proglacial fluvial and lacustrine environments. In: Jopling, A.G., MacDonald, B.C. (Eds.), Special Publication, 23. Society of Economic Paleontologists and Mineralogists, Tulsa, OK, pp. 22–100.
Clague, J.J., 2000. Recognizing order in chaotic sequences of Quaternary sediments in the Canadian Cordillera. Quaternary International 68–71, 29–38.
Fay, H., 2002. Formation of kettle holes following a glacial outburst flood (jökulhlaup) Skeiðarársandur, southern Iceland. In: Snorrason, Á. (Ed.), Extremes of the Extremes: Extraordinary Floods, Proceedings of a Symposium Held in Reykjavik, July 2000. Special Publication, 271. International Association of Hydrological Sciences, Oxfordshire, pp. 205–210.
Fiore, J., Pugin, A., Beres, M., 2002. Sedimentological and GPR studies of subglacial deposits in the Joux Valley (Vaud, Switzerland): backset accretion in an esker followed by an erosive jökulhlaup. Géographie Physique et Quaternaire 56 (1), 19–32.
Fulton, R.J., 1991. A conceptual model for growth and decay of the Cordilleran Ice Sheet. Géographie Physique et Quaternaire 45, 281–286.
Fulton, R.J., Walcott, R.I., 1975. Lithospheric flexure as shown by deformation of glacial lake shorelines in Southern British Columbia. Geological Society of America Memoir 142, 163–173.
Greenwood, S.L., Clark, C.D., 2009. Reconstructing the last Irish Ice Sheet: a geomorphologically-driven model of ice sheet growth, retreat and dynamics. Quaternary Science Reviews 28, 3101–3123.
Hebrand, M., Åmark, M., 1989. Esker formation and glacier dynamics in eastern Skåne and adjacent areas, southern Sweden. Boreas 18, 67–81.
Heginbottom, J.A., 1972. Surficial geology of Taseko Lakes Map Area, British Columbia. Geological Survey of Canada Paper 72-14. Queens Printer, Ottawa, ON, p. 8.
Heinz, J., Aigner, T., 2003. Three-dimensional GPR analysis of various Quaternary gravel-bed braided river deposits (southwestern Germany). In: Bristow, C.D., Jol, H.M. (Eds.), Ground Penetrating Radar in Sediments: Special Publications 211, Geological Society, London, pp. 99–110.
Holland, S.S., 1976. Landforms of British Columbia: a physiographic outline. Geological Survey of Canada Bulletin, 48. Queens Printer, Ottawa ON, p. 138.
Hooke, R.L., Fastook, J., 2007. Thermal conditions at the bed of the Laurentide ice sheet in Maine during deglaciation: implications for esker formation. Journal of Glaciology 53 (183), 646–658.
Huscroft, C.A., 2009. Surficial geology, Criss Creek, British Columbia. Geological Survey of Canada open file 5932, scale 1:50000, Ottawa, ON.
Johnsen, T.F., Brennand, T.A., 2004. Late-glacial lakes in the Thompson Basin, British Columbia: paleogeography and evolution. Canadian Journal of Earth Sciences 41, 1367–1383.

Jol, H.M., Smith, D.G., 1991. Ground penetrating radar of northern lacustrine deltas. Canadian Journal of Earth Sciences 28, 1939–1947.
Kilner, M., West, J.L., Murray, T., 2005. Characterisation of glacial sediments using geophysical methods for groundwater source protection. Journal of Applied Geophysics 57, 293–305.
Kleman, J., Borgstrom, I., 1996. Reconstruction of palaeo-ice sheets: the geomorphological data. Earth Surface Processes and Landforms 21, 893–909.
Kleman, J., Jansson, K., De Angelis, H., Stroven, A.P., Hättestrand, Alm, G., Glasser, N., 2010. North American ice sheet build-up during the last glacial cycle, 115-21 kyr. Quaternary Science Reviews 29, 2036–2051.
Kostic, B., Becht, A., Aigner, T., 2005. 3-D sedimentary architecture of a Quaternary gravel delta (SW-Germany): implications for hydrostratigraphy. Sedimentary Geology 181, 143–171.
Krüger, J., 1984. Clasts with stoss-lee form in lodgement tills: a discussion. Journal of Glaciology 30, 241–243.
Lian, O.B., Huntley, D.J., 1999. Optical dating studies of postglacial aeolian deposits from the south-central interior of British Columbia, Canada. Quaternary Science Reviews 18, 1453–1466.
Lowe, D.R., 1982. Sediment gravity flows: II. Depositional models with special reference to the deposits of high-density turbidity currents. Journal of Sedimentary Petrology 52 (1), 279–297.
Maizels, J., 1979. Proglacial aggradation and changes in braided channel patterns during a period of glacier advance: an alpine example. Geografiska Annaler 61, 87–101.
Maizels, J., 1992. Boulder ring structures produced during jokulhlaup flows—origin and hydraulic significance. Geografiska Annaler 74 (1), 21–33.
Neal, A., 2004. Ground-penetrating radar and its use in sedimentology: principles, problems and progress. Earth-Science Reviews 66, 261–330.
Owen, G., 1997. Origin of an esker-like ridge — erosion or channel fill? Sedimentology of the Monington 'Esker' in southwest Wales. Quaternary Science Reviews 16, 675–684.
Palacky, G.J., 1987. Clay mapping using electromagnetic methods. First Break 5 (8), 295–306.
Pellicer, X.M., Gibson, P., 2011. Electrical resistivity and ground penetrating radar for the characterisation of the internal architecture of Quaternary sediments in the Midlands of Ireland. Journal of Applied Geophysics 75, 638–647.
Plouffe, A., 2009. Surficial geology, Green Lake, British Columbia. Geological Survey of Canada open file 5939, scale 1:50000, Ottawa, ON.
Plouffe, A., Bednarski, J.M., Huscroft, C.A., Anderson, R.G., McCuaig, S.J., 2011. Late Wisconsinan glacial history in the Bonaparte Lake map area, south-central British Columbia: implications for glacial transport and mineral exploration. Canadian Journal of Earth Sciences 48 (6), 1091–1111.
Postma, G., 1990. An analysis of the variation in delta architecture. Terra Nova 2 (2), 124–130.
Postma, G., Nemec, W., Kleinspehn, K.L., 1988. Large floating clasts in turbidites: a mechanism for their emplacement. Sedimentary Geology 58, 47–61.
Price, R.J., 1966. Eskers near the Casement Glacier, Alaska. Geografiska Annaler 48 (3), 111–125.
Reynolds, J.M., 1997. An Introduction to Applied and Environmental Geophysics. John Wiley and Sons, Chichester, England, p. 806.
Rice, S.P., Church, M., Wooldridge, C.L., Hickin, E.J., 2009. Morphology and evolution of bars in a wandering gravel-bed river; lower Fraser river, British Columbia, Canada. Sedimentology 56, 709–736.
Ryder, J.M., 1971. The stratigraphy and morphology of para-glacial alluvial fans in south-central British Columbia. Canadian Journal of Earth Sciences 8, 279–298.
Ryder, J.M., Fulton, R.J., Clague, J.J., 1991. The Cordilleran Ice Sheet and the glacial geomorphology of southern and central British Columbia. Géographie physique et Quaternaire 45 (3), 365–377.
Sambrook Smith, G.H., Ashworth, P.J., Best, J.L., Woodward, J., Simpson, C.J., 2006. The sedimentology and alluvial architecture of the sandy braided South Saskatchewan River, Canada. Sedimentology 53, 413–434.
Shilts, W.W., Aylsworth, J.M., Kaszycki, C.A., Klassen, R.A., 1987. Candian shield. In: Graf, W.L. (Ed.), Geomorphic Systems of North America: Geological Society of America Special Publication, 2, pp. 119–161.
Shreve, R.L., 1985. Esker characteristics in terms of glacier physics, Katahdin esker system, Maine. GSA Bulletin 96, 639–646.
Smith, N.D., Ashley, G.M., 1985. Proglacial lacustrine environment. In: Ashley, G.M., Shaw, J., Smith, N.D. (Eds.), Glacial Sedimentary Environments, SEPM Short Course Notes, 16, Tulsa, OK, pp. 135–216.
Tipper, H.W., 1971a. Multiple glaciation in central British Columbia. Canadian Journal of Earth Sciences 8 (7), 743–752.
Tipper, H.W., 1971b. Glacial geomorphology and Pleistocene history of central British Columbia. Geological Survey of Canada Bulletin, 196. Queens Printer, Ottawa, ON, p. 89.
Tipper, H.W., 1971c. Surficial geology, Bonaparte Lake, British Columbia. Geological Survey of Canada, map 1293A, scale 1:250000, Ottawa, ON.
Warren, W.P., Ashley, G.M., 1994. Origins of the ice-contact stratified ridges (eskers) of Ireland. Journal of Sedimentary Research A64 (3), 433–449.
Winsemann, J., Asprion, U., Meyer, T., Schramm, C., 2007. Facies characteristics of Middle Pleistocene (Saalian) ice-margin subaqueous fan and delta deposits, glacial Lake Leine, NW Germany. Sedimentary Geology 193, 105–129.
Wooldridge, C.L., Hickin, E.J., 2005. Radar architecture and evolution of channel bars in wandering gravel-bed rivers: Fraser and Squamish rivers, British Columbia, Canada. Journal of Sedimentary Research 75, 844–860.